Anisotropic effect of biaxial strain on phosphorus diffusion in silicon

E. Rauls
iNANO and Department of Physics and Astronomy, University of Aarhus, DK-8000 Århus C, Denmark
(Received 31 March 2006; revised manuscript received 24 May 2006; published 15 August 2006)

In $Si/Si_{1-x}Ge_x$ heterostructures, the lattice mismatch induces x-dependent strains in neighboring layers. The effect of such a biaxial strain on the migration of phosphorus dopants in silicon has been investigated theoretically. The interstitial-based diffusion process of phosphorus can be divided into sequences of various migration steps. A clear preference of diffusion along the compressed direction is found. The applied strain has been found to lower the activation energies of most of the discussed steps and thus enhance the overall diffusivity.

DOI: 10.1103/PhysRevB.74.075204 PACS number(s): 61.72.Tt, 66.30.Lw, 62.20.−x, 68.65.−k

I. INTRODUCTION

Dopant diffusion in silicon has been studied intensively during the past decades. The effect of strain, however, first moved into the focus of these studies during the last few years, when moving on to growing heterostructures of different materials. A controlled introduction of strained layers in heterostructures offers a variety of new technological possibilities in the field of semiconductor devices. Among these systems, $Si_{1-x}Ge_x$ and $Si/Si_{1-x}Ge_x$ heterostructures are currently under the most intense experimental[1–4] and theoretical[5] study. In order to be able to control the electronic properties of these new systems, it is important to understand the behavior of common n-type and p-type dopants in all parts of these systems. Especially on the theoretical side, only very few investigations have been carried out on this matter. Only recently, a very detailed both theoretical and experimental study of pressure effects on B and Sb diffusion in Si and Si-Ge alloys was published.[6]

In this work, we investigate the migration of phosphorus in biaxially strained silicon bulk material. Such strain occurs, e.g., when pure silicon is grown on a $Si_{1-x}Ge_x$ substrate. The lattice constant of this substrate induces an anisotropic deformation of the silicon material grown on top of it—i.e., an extension of the lattice vectors in the xy plane and a compression along the z axis (=growth direction [001]).

As found experimentally as well as theoretically, the migration of phosphorus donors in silicon is clearly dominated by an interstitialcy mechanism.[1,7] Depending on the Fermi level, these interstitials are most likely neutral, negatively, or positively charged. During migration, a recharging in order to reduce the activation energy has been considered in several theoretical models.[8] In contrast to dopants whose diffusion is mainly mediated by a vacancy-based mechanism, interstitial-based dopant diffusion mechanisms are most often enhanced by tensile strain, such as, e.g., caused by growth of the material on a substrate with a larger lattice constant.[1,4–6]

This article is organized as follows: In the following section, we briefly describe our computational setup. Section III is dedicated to the results of our calculations. In Sec. III A we first describe geometries and formation energies of the P interstitial, in Sec. III B its on-site rotation. Sections III C and III D, finally, deal with the migration of P interstitials parallel and perpendicular to the compressed crystal direction. In Sec. IV, the findings are compiled and put into the context of long-range diffusion processes. Finally, Sec. V summarizes the work.

II. COMPUTATIONAL

We performed density functional calculations with the self-consistent charge density functional based tight binding (SCC-DFTB) method.[9] Silicon bulk material was modeled in a $(3\times3\times3)$ supercell containing 216 atoms[10] for all calculations. All atoms but 16 Si atoms at the borders of the unit cell were allowed to relax in all calculations. After having fully relaxed the initial and final configurations, we calculated the migration paths using the constrained relaxation algorithm described in Ref. 11. No certain pathway was assumed in the beginning. Details about this procedure can, e.g., be found in Ref. 12.

Focusing on the diffusion of phosphorus in pure Si-bulk material, the influence of adjacent $Si_{1-x}Ge_x$ layers has been considered by varying the lattice constants of the Si-bulk supercell according to experimental data[13]—i.e., expansion in the xy plane and contraction in the z direction which is supposed to be the surface normal during the growth of a $Si/Si_{1-x}Ge_x$ heterostructure. The strength of these deformations depends on the Ge content x in the substrate. It has been shown in Ref. 13 that the Poisson law is valid over the whole range of x, provided a certain minimum thickness of the silicon layer.[14]

III. RESULTS

In the uncompressed case, our calculations of the optimized Si-bulk structure (i.e., $x=0$) yield a lattice constant of 5.428 Å. A Ge content of 29.9% enlarges the in-plane lattice constant by a factor of 1.0114, while the lattice constant perpendicular to the plane (denoted as the z direction in the following) has to be multiplied by a factor of 0.9912. For 100.0% Ge content in the substrate, these factors become 1.0384 (in plane) and 0.9714 (out of plane).[13] The lattice constants are summarized in Table I. For these three cases (x=0%, 29.9%, 100.0%), we have investigated various migration mechanisms of P interstitials for the neutral-, positive-, and negative-charge states.

The P interstitial exhibits a near-midgap donor level (around 0.5 eV above the valence band edge) and an accep-

 ©2006 The American Physical Society

TABLE I. Lattice constants and binding energies (in [eV]) for $P_{\parallel}$ and $P_{\perp}$ compared to a Si interstitial and a substitutional built-in P atom in neutral- and positive-charge states.

%Ge	Lattice constant	Charge=−1		Charge=0		Charge=+1	
	$a_{\parallel z}/a_{\perp z}$	$P_{\parallel}$	$P_{\perp}$	$P_{\parallel}$	$P_{\perp}$	$P_{\parallel}$	$P_{\perp}$
0	5.428/5.428	2.4	2.4	1.4	1.4	0.4	0.5
29.9	5.380/5.490	1.8	2.1	1.0	1.2	0.2	0.5
100.0	5.273/5.636	0.6	0.9	0.2	0.9	0.0	0.7

tor state close to the conduction band edge. While in the neutral-charge state the donor level is occupied with one electron, both the acceptor and donor levels are unoccupied in the positive-charge state. In general, larger differences in the geometries can, therefore, be expected to be found between the neutral- and positive-charge states. Occupying the near-midgap level with a second electron, as is the case in the negative-charge state, will, in contrast, not lead to strong qualitative differences. In most of the detailed discussions of the geometries, we therefore limit ourselves to the description of the neutral- and/or positive-charge state.

In contrast to the geometry, the electronic structure is affected more strongly by the additional electron. Since the acceptor level is shifted closer to or into the conduction band during some of the migration processes, these mechanisms do not exist and migration requires a recharging.

An accurate investigation of the rather delicate electronic structure of the migrating negatively charged P interstitial requires a more sophisticated method such as, e.g., used for the investigation of the electronic structures of defects in Refs. 12, 15, and 16. It is, however, currently not possible to calculate the defects under investigation in this work within this method. We therefore leave this as a future task.

A. Geometry of the P interstitial

In its most stable configuration, the neutral (and the simply negatively charged) P interstitial shares a site with a silicon atom, where both atoms are moved out of their symmetry planes, compare Figs. 1(b) and 1(e) [or Figs. 1(a) and 1(d) for the negative-charge state, respectively]. The interstitial has a prominent axis, which is tilted against the lattice

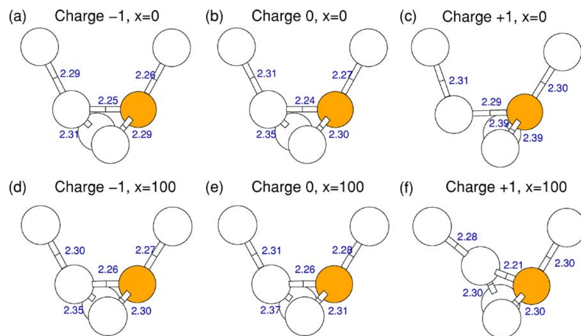

FIG. 1. (Color online) Most stable configuration of the P interstitial for $x=0$ [(a)–(c)] and $x=100$ [(d)–(f)] in the negative-, neutral-, and positive-charge states.

directions. The four Si ligands shown in Fig. 1 are displaced from their lattice sites, as well. The local geometry, however, does not change considerably with the strain induced by a Ge content x, but distortion is rather blurred out over several atomic distances, making the use of a sufficiently large supercell clear, once more (compare also the discussion of Fig. 3 in the following section). In the positive-charge state, a similar configuration has the lowest energy for $x=100$ [compare Fig. 1(f)], while for $x=0$ (and also for $x=29.9$, not shown) a configuration with C_{1h} symmetry has a slightly lower energy [compare Fig. 1(c)]. As is well known, silicon has a very flat potential energy surface, resulting in a large number of local minima for defect configurations. In the given case, several only slightly differing configurations of the defect with energy differences all below 0.1 eV can be found, making a statement of the exact geometry extremely difficult. The same holds for the calculated energies, why the given numbers should not be overestimated but regarded with an error bar of ≈0.1 eV. Nevertheless, allowing for even this large error bar, conclusions do not change. Considering now the most general—i.e., unsymmetric—configuration as found for the neutral-charge state, we can find the defect in 12 (2×6) possible orientations.

In reasonable agreement with previous calculations in a 64-atom supercell,[8] we find a binding energy of 1.4 (0.4) eV for the P interstitial compared to a system with a Si interstitial and a substitutionally built-in phosphorus atom in the neutral- (positive-) charge state. Table I summarizes the values of these binding energies for the various strains applied to the system and the two principally different orientations of the defect axis (mainly) parallel or (mainly) perpendicular to the compressed direction z. In the following, these two orientations of the interstitial will be denoted $P_{\parallel}$ and $P_{\perp}$. Raising the Ge content leads to a destabilization of the neutral- or negative-charge P interstitial for the benefit of the system with the substitutional phosphorus and a Si interstitial. In the case of a pure Ge substrate, the binding energy of 1.4 eV for the neutral P interstitial (in both orientations) is lowered by 85% for $P_{\parallel}$ and 35% for $P_{\perp}$. Similarly, for the negative-charge interstitial, the high binding energy of 2.4 eV for $x=0$ decreases by 75% for $P_{\parallel}$ and 62% for $P_{\perp}$. For the positive-charge state, $P_{\parallel}$ is also destabilized with increasing x. The binding energy is considerably lower than in the neutral-charge state. In contrast to the neutral- or negative-charge state, $P_{\perp}$ gets slightly stabilized with increasing x, while $P_{\parallel}$ is further destabilized. From these results, independent from the Fermi level, the equilibrium distribution of interstitials in all orientations is changed in favor of a higher concentration of $P_{\perp}$ in the strained structures.

Starting from one given position and orientation, the P interstitial can start its migration process either in the xy plane or along the (compressed) z axis ($z=[001]$, upright in all figures). Before discussing the real *migration* mechanisms themselves, we take a closer look at the mobility of the defect on the site, which is an important brick in the complete diffusion process. The on-site rotation of the interstitial allows the defect to change between different directions and mechanisms of migration and might also play a role in potential recharging processes during migration.

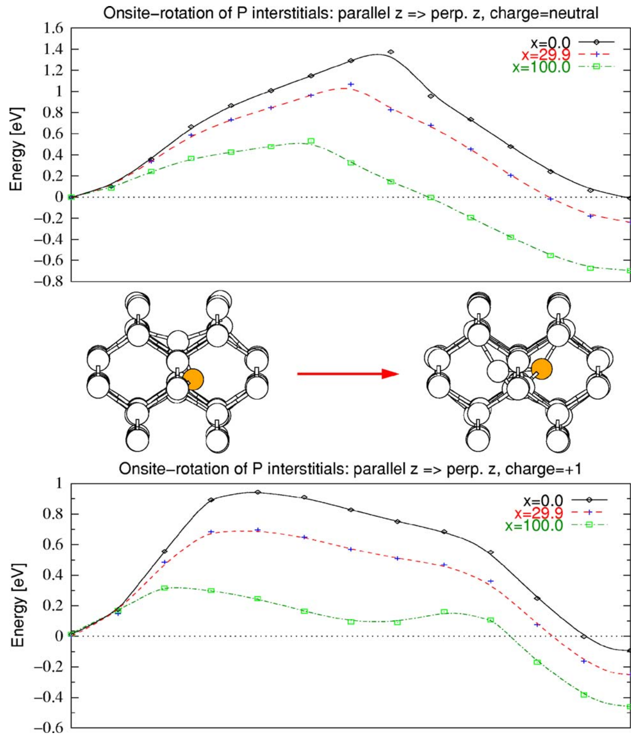

FIG. 2. (Color online) On-site turn of the P interstitial. Increasing tensile strain stabilizes the orientation with the defect axis perpendicular to the compressed z axis for both the neutral- and positive-charge states.

B. On-site rotation of the P interstitial

Two of the 12 possible orientations of the asymmetric P interstitial are in each case connected via a flipping mechanism, which will be discussed later on. Between the remaining six, a turning movement is required. Their investigation can be reduced to the rotational movement which leads the interstitial from a $P_{\parallel}$ to a $P_{\perp}$ configuration.

This is illustrated in Fig. 2. If the strain is applied as described above, one crystal direction (along the z axis) becomes different from the others, so that the four possible orientations of the defect perpendicular to this axis get different energies than those two that are (mainly) parallel to the compressed axis. The diagrams in Fig. 2 show that for the strain induced by increasing Ge content x, the orientations perpendicular to the compressed axis are stabilized over the orientation parallel z for both charge states. Upon straining the structures, the rotational energy barriers to get from $P_{\parallel}$ to the more stable $P_{\perp}$ are strongly reduced: for $x=100$ by 58% (74%) for the neutral- (positive-) charge state. The barrier for the back rotation is considerably less affected; i.e., the strain causes a real stabilization instead of an enhancement of the rotation, only. The values for the energy barriers are summarized in Table II.

Especially for those configurations of the positive-charge state which have C_{1h} symmetry, another type of on-site rotation is important for long-range diffusion processes. A rotation of 90° within the xy plane (perpendicular to the compressed axis) mediates between two isoenergetic orientations of these configurations. As shown in Secs. III D and IV, alternation between these two configurations is part of a possible in-plane diffusion mechanism. For $x=0$, the rotation can be activated with 1.21 eV; for $x=29.9$, the activation energy is slightly lower, 1.10 eV, and for $x=100$, 1.05 eV are required to activate this rotation (see Table II and Fig. 3). Since the activation energy for back rotation from $P_{\perp}$ to $P_{\parallel}$ is lower by ≈0.2 eV, in-plane rotation will rather be realized in two steps via the parallel position as an intermediate state. Below the energy diagram in Fig. 3, the geometries of the initial, saddle point, and final orientations of the interstitial are shown, viewed along the (compressed) axis. In this perspective, it can nicely been seen how far the distortion of the lattice is spread around the defect, especially along the direction parallel to the defect axis. This observation was similarly made for an isolated vacancy[16] and emphasizes, again, the importance of using a supercell of at least the size shown in Fig. 3.

TABLE II. Summary of the energy barriers (in eV) for the on-site rotation of the P interstitial for different Ge contents x and charge states: $(P_{\parallel}\rightarrow P_{\perp})/(P_{\perp}\rightarrow P_{\parallel})$.

%Ge	−1	Neutral	"+1"	In-plane ("+1")
0	3.0/3.0	1.30/1.30	0.93/1.04	1.21
29.9	2.68/2.97	1.09/1.33	0.70/0.95	1.10
100.0	1.19/2.11	0.55/1.24	0.24/0.78	1.05

For the negative-charge state, the rotational transition from $P_{\parallel}$ to $P_{\perp}$, as described for the neutral- and positive-charge states, does most likely not exist for small values of x. In Fig. 4, the energy curves for the three different values of x are shown. For the given process unphysically high-energy barriers obtained for $x=0$ and $x=29.9$, however, give a hint that these processes do not exist for this charge state. The reason might be found in the electronic structure of the saddle point configurations of these processes. For these, the highest occupied level is strongly localized at the P atom. For the smaller values of x, this level moves, however, across the conduction band edge, meaning that the configuration does

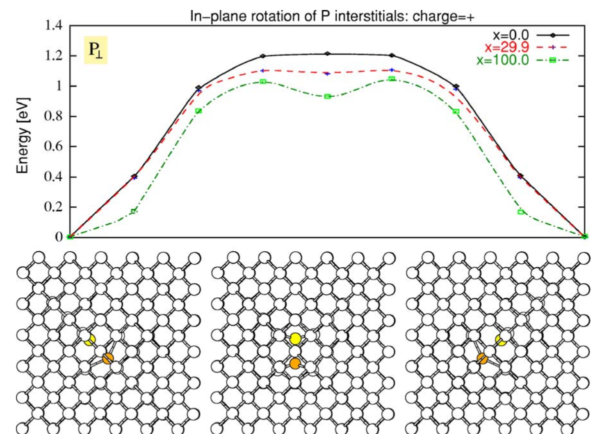

FIG. 3. (Color online) In-plane rotation of the positive-charged P interstitial. Below, the initial, saddle point, and final geometries are shown in a top view along the (compressed) axis to demonstrate the extended lattice distortion.

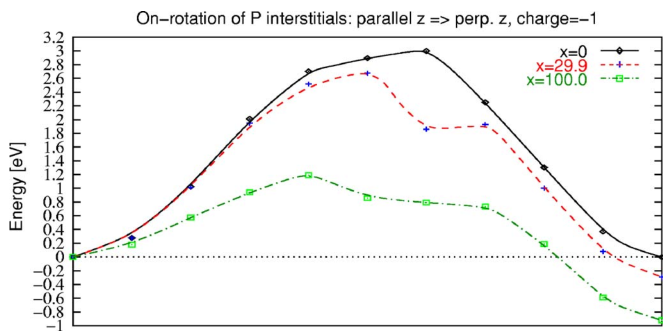

FIG. 4. (Color online) On-site turn of the P interstitial in the negative-charge state.

not exist. For $x=100$, the level is pushed down by nearly 0.2 eV, so that it comes to lie in the band gap. Therefore, the activation energy for the rotation increases rather continuously with the charge state from "+1" to "−1" for $x=100$. For $x=0$ and $x=29.9$, in contrast, an unphysical jump to high activation energies is seen (compare Table II).

For small x, it is therefore likely that rotation of the P interstitial can take place via a recharging process from "−1" to neutral, only.

C. Migration parallel to the compressed axis

Induced by the asymmetric geometry of the interstitial, all migration processes can be divided into two parts: a flipping movement and "real migration step". In the flipping step, the interstitial does not change the lattice site, but only the tilting axis of the P-Si is reoriented (left part in Fig. 5). In the real migration step, the P atom moves on to a nearby Si site (right part in Fig. 5). Together, these two steps determine a continuous long-range diffusion of the P atom through the Si lattice.

For an orientation of the defect axis parallel to the compressed z axis, the mechanism is depicted in Fig. 5(a). The first step shows the flipping, while the second step illustrates the "moving step," which leads the P atom to a position shared with the ligand of its initial position. In Figs. 5(b) and 5(c) the change in energy during these two steps is shown for the neutral- and positive-charge states, respectively. In both charge states the flipping of the defect axis requires approximately the same activation energy—i.e., 0.6 eV (0.7 eV) for the neutral- (positive-) charge state [compare left part of the curves in Figs. 5(b) and 5(c) and columns 2 and 3 in Table III]. An applied strain obviously hardly affects this process. The moving step has a considerably higher activation energy and is, therefore, the rate-determining part of the migration process. In contrast to the flipping step, applied strain strongly affects the activation energy of this step: The right part of the curves in Figs. 5(b) and 5(c) show the strong reduction of the energy barrier by 39% for the neutral- and 44% for the positive-charge state. The initial, saddle point, and final geometries of this moving step are shown in Fig. 5(e). In the saddle point geometry, Si atom 1 can form a bond to Si atom 3 (yet being far from sp^3 configuration), while the phosphorus atom can bind to Si atom 5. The whole structure is strongly deformed, and first after the stepwise bond for-

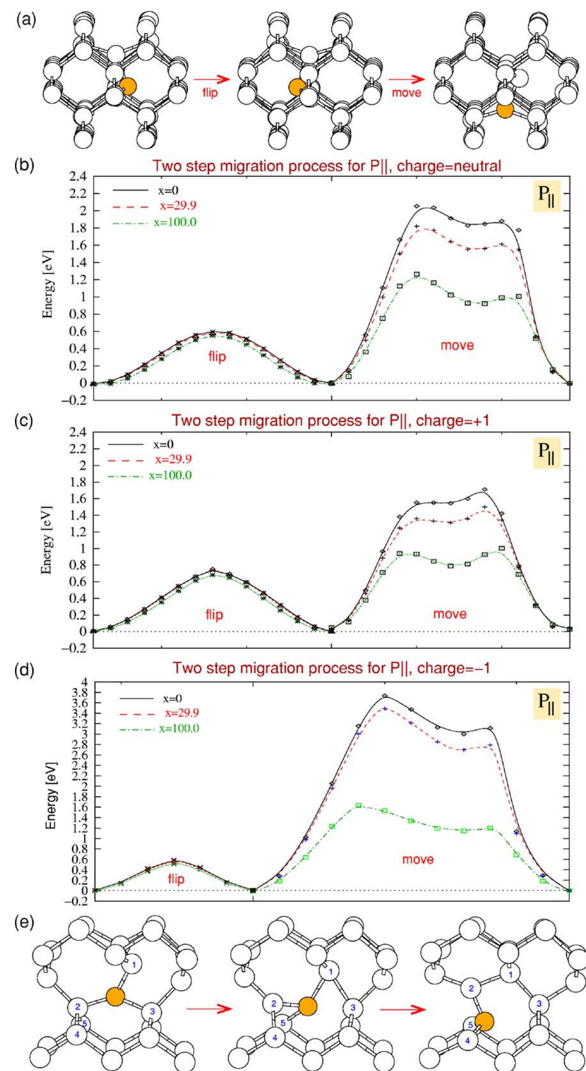

FIG. 5. (Color online) Migration of $P_{\parallel}$ along the z axis in two steps as shown in panel (a). Energy curves for the neutral- (b), positive- (c), and negative- (d) charge states. Panel (e) shows details of the moving step.

mation between Si atoms 1 and 2 on the one hand and the P atom and Si atom 4 on the other hand, the energy strongly decreases until the final geometry is reached. The bond lengths do not vary much with x. The distance between Si atom 1 and 3 is 2.47 Å for $x=0$ and 2.46 Å for $x=100$, and the bond lengths between the P atom and Si atoms 2 or 5 are 2.19 (2.20) and 2.44 (2.45) for $x=0$ ($x=100$). Nor for the positive-charge state was a qualitative difference in the mechanism found (as is the case for the perpendicular direction). The distance between Si atom 1 and 3 is 2.38 Å for $x=0$ and 2.36 Å for $x=100$, and the bond lengths between the P atom and Si atoms 2 or 5 are 2.17 (2.19) and 2.47 (2.48) for $x=0$ ($x=100$). The negative-charge state shows, as in the case of the on-site rotation, some special features. As shown in Fig. 5(d), all we said about the flipping part of the mechanism upon discussing the neutral- and positive-charge state holds also in this case. The activation energies for the flipping are only slightly lower as for "0" and "+1" and decrease slightly with x (compare Table III). The moving

TABLE III. Activation energies (in eV) for migration along z: comparison for the two different orientations of the defect axis for the different Ge contents x and the three charge states.

%Ge	Defect axis $\parallel z$		Defect axis $\perp z$	
x	flip $-/0/+$	move $-/0/+$	flip $0/+$	move $-/0/+$
0.0	0.58/0.60/0.75	3.74/2.06/1.72	0.78/0.80/0.78	2.34/1.32/1.36
29.9	0.56/0.58/0.75	3.49/1.82/1.47	0.74/0.77/0.73	2.36/1.40/1.42
100.0	0.53/0.56/0.68	1.63/1.26/0.97	0.64/0.63/0.60	2.00/1.47/1.56

part of the migration mechanism, however, seems to suffer from similar problems in the electronic structure as discussed in Sec. III B for the on-site rotation. For $x=100$, the mechanism runs analogously to the other two charge states and can be activated with 1.63 eV. For $x=0$ and $x=29.9$, however, an apparently nonexisting saddle point configuration has to be passed. In this case, migration should, thus, only be possible by recharging to the neutral state, in case of which the saddle point configuration exists.

Similarly, $P_\perp$ can migrate along the compressed direction as illustrated in Fig. 6(a). The migration can, again, be divided into a flipping and a moving part, for which the energy diagrams for the neutral-, positive-, and negative-charge states are shown in Figs. 6(b)–6(d). Activation energies for the flipping process are comparable to those for $P_\parallel$ discussed above. Also their reduction with increasing x is comparable. The moving step, in contrast, can be activated with much lower energies than in case of $P_\parallel$. At the saddle point, the P atom takes the configuration shown in Fig. 6(e). In the neutral-charge state and for $x=0$, the bonds from the P atom to its two Si ligands (marked with 1 and 2) are 2.2 Å. These two Si atoms change from a threefold to a twofold coordination (Si 2) and vice versa (Si 1). In the shown structure, the two short bonds of Si 2 are 2.25 and 2.30 Å; the distance to the third Si is 2.89 Å. The bonds of Si 1 are 2.33, 2.35, and 2.40 Å, respectively. For $x=100$, the mechanism is the same and the bonds are of comparable lengths. The slight increase of 11% (15%) in the activation energy for this process might be due to stronger local distortions—i.e., stronger variations of the bond angles around the Si ligands from the ideal tetrahedral angles. In unstrained Si, only 1.32 (1.36) eV are needed to activate this step in the neutral- (positive-) charge state, compared to 2.06 (1.72) eV for $P_\parallel$ (compare columns 4 and 5 in Table III). Since the activation energy for the moving step is not reduced in this case but, in contrast, strong in the case of a parallel orientation, a raising of x causes the activation energy for the movement of $P_\parallel$ to become lower than that for the movement of $P_\perp$ (see Table III).

D. Migration perpendicular to the compressed axis

With the mechanisms described up to now, the P atom is transported along the (compressed) z axis. In this section, we will discuss mechanisms for the migration perpendicular to this direction. For $P_\perp$, a possible mechanism is depicted in Fig. 7. As shown for the symmetrical configuration of the positive-charge state, the movement includes a 90° rotation of the interstitial.

For the unsymmetric configurations, an additional flipping step (not shown in Fig. 7) is needed. As in the cases discussed before, the activation energy for this step is only slightly affected by the applied strain (compare columns 5 and 6 in Table IV). As in the first case discussed, the activation energies are lowered upon increasing x. For $x=100$, the

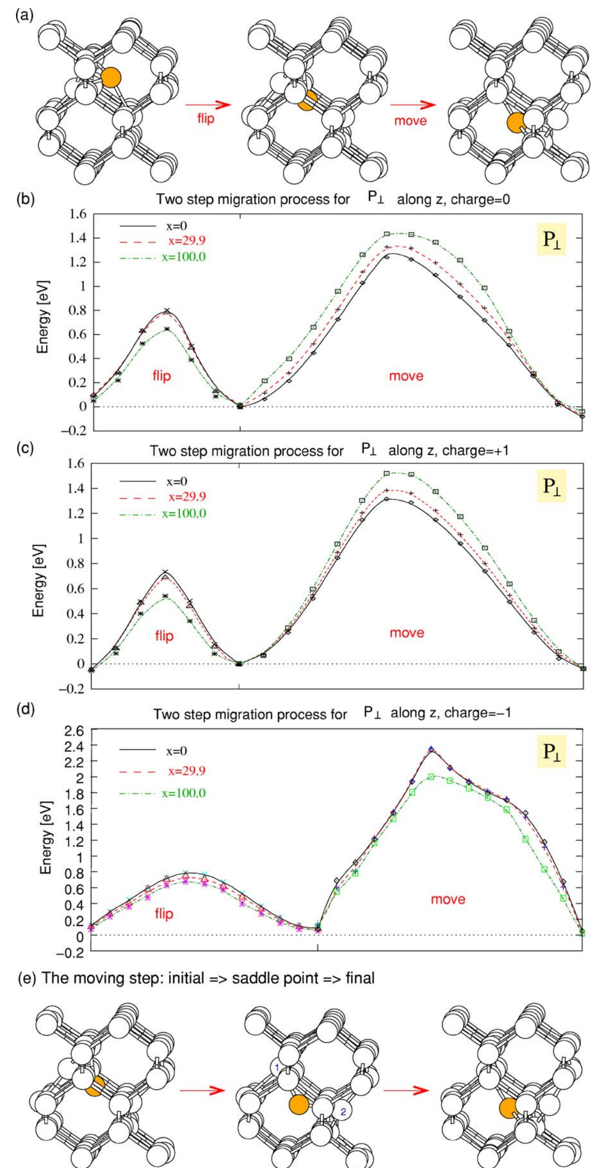

FIG. 6. (Color online) Migration of the $P_\perp$ along the z axis. The activation energy increases slightly with the Ge content x.

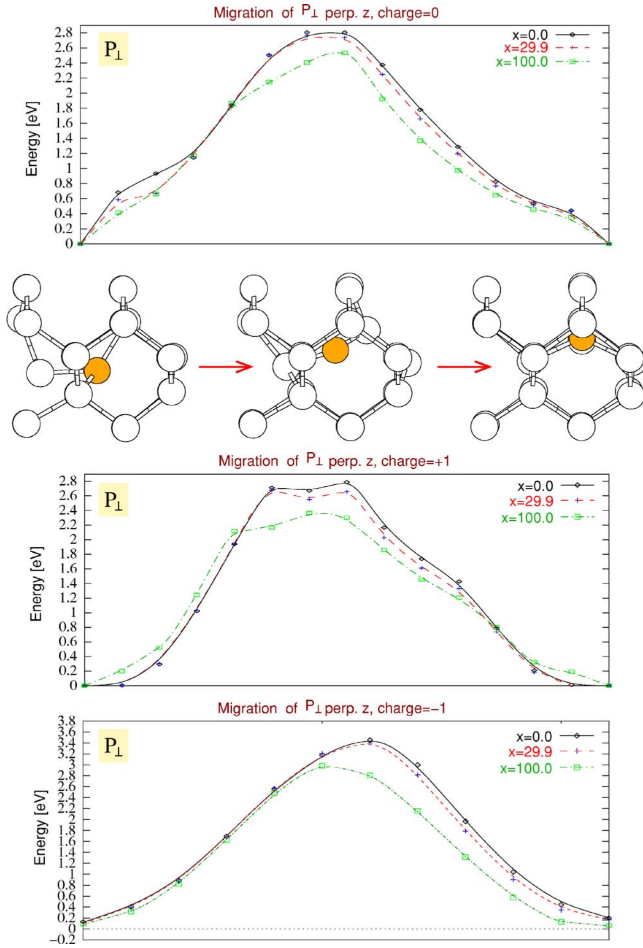

FIG. 7. (Color online) Migration of $P_\perp$ perpendicular to the z axis. The activation energy decreases slightly with the Ge content x.

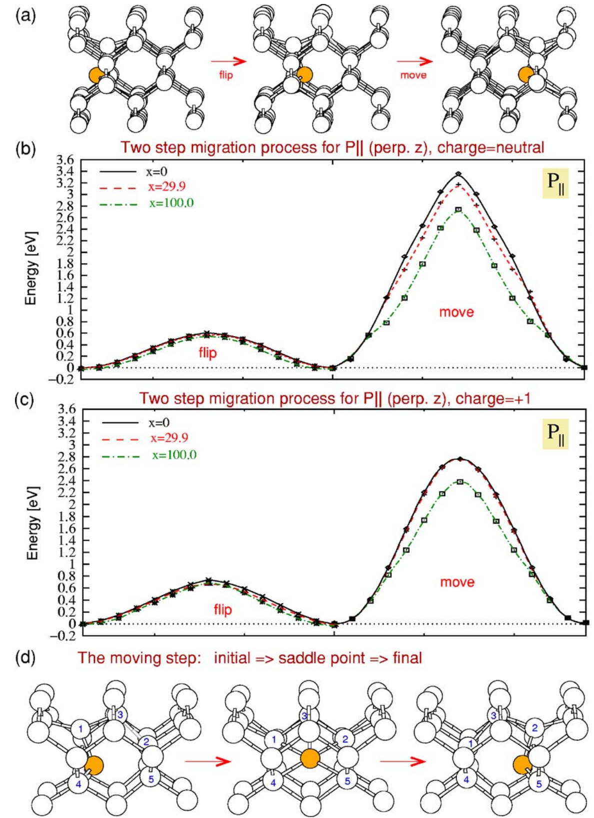

FIG. 8. (Color online) Migration of $P_\parallel$ perpendicular to the z axis in two steps as shown in panel (a). Energy curves for the neutral- (b) and the positive- (c) charge state. Panel (d) shows details of the moving step.

moving barriers are reduced by about 30% for all charge states.

For $P_\parallel$, two mechanisms for the migration perpendicular to the z axis are discussed by means of Figs. 8 and 9. Again, a flipping step is needed between the moving steps, for which a longer, symmetric step is conceivable as shown in Fig. 8. Alternatively, migration could run via a two-step process (thus including twice as much flipping steps) as shown in Fig. 9. Here, the P atom just moves to a ligand site, while it directly moves to a next-nearest-neighbor site in the first named mechanism.

In the latter, the strain induced by a pure Ge layer lowers the activation energy for this moving step by 18% in the neutral- and 13% in the positive-charge state (see Fig. 8). The atomic configurations of the initial, the saddle point, and the final geometries are shown in Fig. 8(d). The P interstitial induces a strong reordering of the surrounding Si atoms. On the way from the initial geometry to the saddle point, the strong displacement of Si atom 1 decreases, while that of Si atom 2 gradually increases, and the bonds to Si atom 5 and the one behind it are loosened. Si atom 1 lowers its energy meanwhile by reforming bonds to Si atom 4 and the one behind. The saddle point geometry has a mirror plane, and the P atom forms four rather long bonds to Si atoms 1,2 ($x=0$, 2.55 Å; $x=100$, 2.59 Å) and 4,5 ($x=0$, 2.50 Å; $x=100$, 2.57 Å). A shorter bond ($x=0$, 2.42 Å; $x=100$, 2.36 Å) is additionally formed to Si atom 3. In contrast to the four weaker bonds to atoms 1,2,4,5, this bond is, thus, slightly

TABLE IV. Activation energies (in eV) for migration perpendicular to z: comparison for the two different orientations of the defect axis for the different Ge contents x and the two charge states. For $x=0$ or $x=29.9$, the interstitial is symmetrical in the positive-charge state; thus no flip is needed.

%Ge	Defect axis $\parallel z$			Defect axis $\perp z$	
x	flip 0/+	move (1) 0/+	move (2) −/0/+	flip 0/+	move 0/+
0.0	0.60/0.75	3.36/2.75	3.35/2.85/2.89	0.58/–	2.80/2.79
29.9	0.58/0.75	3.17/2.74	3.33/2.54/2.83	0.61/–	2.76/2.65
100.0	0.56/0.68	2.74/2.38	2.28/1.94/1.78	0.49/0.33	2.55/2.36

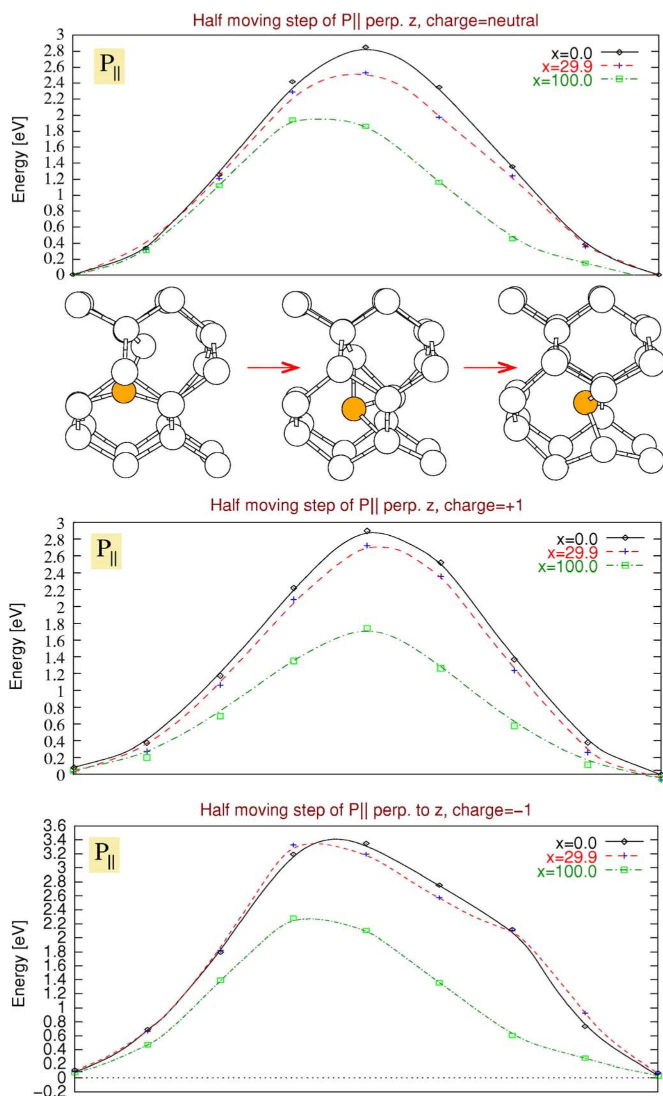

FIG. 9. (Color online) Migration of $P_{\|}$ perpendicular to the z axis: alternative mechanism for the move step from Fig. 8. P moves only half the way, thus requiring an additional flip.

strengthened due to the compression of the lattice in the z direction, which might contribute to the stabilization of the saddle point structure for higher x. For the positive-charge state, the effect of x on the four long bonds is similar: The bonds to atoms 1,2 (4,5) elongate from 2.40 (2.49) Å for $x=0$ to 2.51 (2.66) Å. In contrast to the neutral-charge state, however, the distance from the P atom to Si atom 3 is with 2.90 Å for $x=0$ (2.54 Å for $x=100$) too large to support a stabilization of the saddle point structure, which might explain the smaller effect in this charge state.

Following, alternatively, the mechanism depicted in Fig. 9, the P atom is moved only very little, but an amount of energy similar to the previously described process has to be brought up to displace the surrounding Si atoms. At the saddle point, in the $x=0$ case, two bonds (2.38 and 2.43 Å) are formed between the P atom and the Si atoms which share their sites with the P atom in the respective initial or final geometry. For $x=0$, one more short P-Si bond is formed ($x=0$, 2.19 Å) in direction of the initial position. For $x=100$, the geometry is slightly more symmetric; i.e., two bonds are formed to Si atoms of each of the initial (2.21 and 2.45 Å) and final (2.39 and 2.56 Å) geometries.

In both moving mechanisms, the applied strain lowers the activation energy for the process. The activation energy for the long moving step is decreased by 18% (13%), and a stronger reduction is found for the short step, namely, 32% for both the neutral- and negative-charge state and 38% for the positive-charge state, respectively. For low x, the longer moving step is slightly preferred in the positive-charge state; otherwise, activation energies are clearly lower for the short step.

IV. DISCUSSION

In all described processes, where the P atom changes its site, one Si atom—namely, the one that shares its site with the phosphorus atom—releases its deflection, while another Si atom is displaced by the same amount. In the neutral (positive) charge state, this displacement amounts to 0.65 (0.62) Å for $x=0$ and 0.64 (0.62) Å for $x=100$. The absolute difference due to the different Ge contents x is only small in the neutral- and nearly not detectable in the positive-charge state. Considering, however, the changed bond lengths in the strained Si lattice, it becomes more clear. In pure silicon—i.e., $x=0$—the Si-Si bond length in our calculations is 2.35 Å. In the strained lattice with $x=100$, this bond length is elongated by 1.6% to 2.387 Å. Expressed relative to these usual bond lengths in the lattice, the displacement of the Si atom due to the P interstitial in the neutral- (positive-) charge state is 27.5% (26.5%) for $x=0$ and 26.6% (25.9%) for $x=100$. The effort of the P atom to deform the surrounding lattice is, thus, nearly 1% less in the strained structure, which contributes to the lower activation energies found for these structures. This interpretation is further reinforced by the observation that the activation energies for the various flipping processes, in which only the P atom moves, are hardly affected by the strain.

In order to compile the obtained data for the single steps and use them to build up a model for long-range diffusion processes, we have collected the most important findings and put them together in a more schematic overview. For both the neutral- and positive-charge states, Fig. 10 shows the values of the activation energies for the most favorable flipping, rotation, or moving mechanisms schematically for the two limiting cases of growth on a pure Si substrate ($x=0$, top two diagrams), and a pure Ge substrate, ($x=100$, bottom two diagrams).

The negative-charge state has been omitted from these reconsiderations, because the inclusion of the most likely necessary recharging processes in the case of several of the discussed mechanisms only would complicate the picture. Since it in all these cases anyway gives the requested information, the neutral charge state should be taken as a "substitute."

Assuming the phosphorus to be built in during growth (as is the case in, e.g., the experiments in Ref. 13), we will find P interstitials of all orientations equally distributed for unstrained, pure Si (compare the results from Sec. III A). For

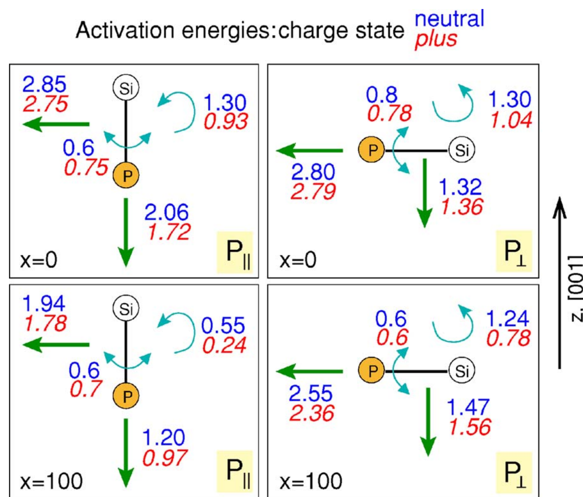

FIG. 10. (Color online) Schematic summary of the most important activation energies for $P_{\parallel}$ (left column) and $P_{\perp}$ (right column). Values for $x=0$ are shown in the first row, for $x=100$ in the second row. Upper (blue) values are for the neutral-, bottom (red) values for the positive-charge state.

$x=100$, however, the greatest amount of P interstitials will be built in with the defect axis in the strained xy plane. Combining the numbers given in Fig. 10, we can now compare which mechanisms are possible for a given amount of energy. Say, the interstitials are in the neutral-charge state, and we have slightly above 1.3 eV of energy available. For $x=0$, we can then activate a rotation between the parallel and perpendicular orientations. Furthermore, $P_{\perp}$ can be activated to move along the z axis. The migration mechanisms in the xy plane, however, require much higher energies to be activated. For $x=100$, we can, similarly, activate the rotation. Migration along the z axis can be activated in two steps: first rotation to the parallel orientation, then migration of the resulting $P_{\parallel}$ along z. Going slightly up with the available energy—say, to $\approx$1.5 eV—migration in this direction can also be activated directly for $P_{\perp}$. Diffusion in this direction can, therefore, be expected to become more likely. For $x=0$, no further mechanisms can be activated at this energy. Raising the available energy to $\approx$1.8 eV, the migration of $P_{\parallel}$ along z might become possible, as well—provided the actual position of the Fermi level allows a recharging during the process, so that only the lower energy of the positive-charge state has to be overcome. In that case, the migration of $P_{\parallel}$ perpendicular to the z axis can be activated for $x=100$. Finally, an energy of $\approx$2.6 eV is sufficient to activate all the discussed mechanisms for the P interstitial for $x=100$. In the unstrained case, an $\approx$0.3 eV higher energy is needed for that. If the defects are positively charged from the beginning, the picture is similar; only activation energies are lower in most cases. The difference between the strained and unstrained structures, however, remains unchanged.

The applied strain facilitates most of the possible migration mechanisms of P interstitials and thus also their complete diffusion process. Since at higher Ge contents x more mechanisms become allowed already in the energy range between 1.5 and 1.8 eV, diffusion can be expected to be enhanced compared to the pure silicon. Another effect of the strain might be a more uniform distribution in the xy plane due to lower migration energy barriers for this direction. However, migration along the (compressed) z axis is clearly preferred over migration perpendicular to it. If thinking of heterostructures, one might, in particular for increasing x, expect an increasing diffusion of the P interstitials into the (in the z direction) neighboring $Si_{1-x}Ge_x$ layer. In experimental studies of the diffusion of P in $Si_{1-x}Ge_x$, it has been observed[1] that phosphorus diffuses faster with increasing x and, in addition, increasingly segregates towards the Si side with increasing x. The increasing x might, thus, lead to a phosphorus accumulation near the interface on both sides. This depends, though, on the influence of the interface structure itself as well as—considering the long-range distortion of the silicon lattice—the influence of other P defects, in both mobile and built-in forms in this region. These questions have to be subject to further investigations.

V. CONCLUSION

Summarizing, various mechanisms of rotation and reorientation as well as migration of P interstitials in unstrained and strained silicon bulk have been investigated by density functional theory calculations. Upon combining these steps, long-range diffusion pathways can be constructed. The most important findings of these investigations are first that, in strained material, the interstitial preferably orients its axis perpendicular to the compressed axis ($P_{\perp}$). Second, migration is strongly favored along the compressed direction. The applied strain facilitates most of the discussed steps. Most mechanisms have lower activation energies in the positive- than in the neutral-charge state. A recharging process, as proposed in various previous works on the subject, is therefore very likely if allowed by the position of the Fermi level. For the negative-charge state, some of the migration mechanisms that were found for the neutral- and positive-charge states do apparently not exist for low x values. In these cases, a recharging process becomes, therefore, necessary for the mobility of the P interstitial.

It remains a future task to investigate the consequences of the expected effect of accumulation of phosphorus at the interface for the electronic properties of $Si/Si_{1-x}Ge_x$ heterostructures. In addition, the influence of the layer thickness on this effect has to be investigated, since the interstitial might exhibit a considerably different behavior in only few-layer-thick silicon (and $Si_{1-x}Ge_x$) than in the here presented bulk investigations. In subsequent theoretical work on this matter, the atomistic structure of the interface should be modeled explicitly. Molecular dynamics simulations might, furthermore, be useful in this context.

[1] J. S. Christensen, H. H. Radamson, A. Y. Kuznetsov, and B. G. Svensson, J. Appl. Phys. **94**, 6533 (2003).
[2] H. Bracht, MRS Bull. **25**, 22 (2000).
[3] Y. Zhao, M. J. Aziz, N. Zangenberg, and A. N. Larsen, Appl. Phys. Lett. **86**, 141902 (2005).
[4] A. N. Larsen, N. Zangenberg, and J. F. Pedersen, Mater. Sci. Eng., B **124-125**, 241 (2005).
[5] S. T. Dunham, M. Diebel, C. Ahn, and C. Shih, J. Vac. Sci. Technol. B **24**, 456 (2006).
[6] M. J. Aziz, Y. Zhao, Hans-J. Gossmann, S. Mitha, S. P. Smith, and D. Schiferl, Phys. Rev. B **73**, 054101 (2006).
[7] A. Ural, P. B. Griffin, and J. D. Plummer, J. Appl. Phys. **85**, 6440 (1999).
[8] X. Liu, W. Windl, K. Beardmore, and M. Masquelier, Appl. Phys. Lett. **82**, 1839 (2003).
[9] Th. Frauenheim, G. Seifert, M. Elstner, Z. Hajnal, G. Jungnickel, D. Porezag, S. Suhai, and R. Scholz, Phys. Status Solidi B **217**, 41 (2000).
[10] As shown in Ref. 16, for the description of defects in silicon, the use of a largely extended supercell clearly has to be preferred over a smaller cell with a larger *k*-point set.
[11] M. Kaukonen, P. K. Sitch, G. Jungnickel, R. M. Nieminen, S. Pöykkö, D. Porezag, and Th. Frauenheim, Phys. Rev. B **57**, 9965 (1998).
[12] U. Gerstmann, E. Rauls, Th. Frauenheim, and H. Overhof, Phys. Rev. B **67**, 205202 (2003).
[13] Lattice deformation according to experimental data obtained by M. Huebl, A. R. Stegner, M. Stutzmann, M. Brandt, G. Vogg, F. Bensch, E. Rauls, and U. Gerstmann, Phys. Rev. Lett. (to be published 2006). The validity of Poissons law in this case has been shown in theory and experiment.
[14] Calculations with the same method as used in this work show the validity of the Poisson law for Si slabs of the same thickness as the supercell used in this work.
[15] U. Gerstmann, E. Rauls, H. Overhof, and Th. Frauenheim, Mater. Sci. Forum **483-485**, 465 (2004).
[16] U. Gerstmann, E. Rauls, H. Overhof, and Th. Frauenheim, Phys. Rev. B **65**, 195201 (2002).